BRIEF NOTE

Microscopic fractures shown inside tablets after impact

Japanese Journal of Applied Physics **63**, 028005 (2024) **BRIEF NOTE**
https://doi.org/10.35848/1347-4065/ad21be

Microscopic fractures shown inside tablets after impact

Craig S. Carlson[1,2*], Michiel Postema[1,2], Nicole Anderton[1], Markus Hannula[1], Joona Sorjonen[3], Hu Xinyue[4], Naoyuki Otake[4], Nobuki Kudo[4], Jari Hyttinen[1], and Jarkko Ketolainen[3]

[1]*BioMediTech, Faculty of Medicine and Health Technology, Tampere University, Korkeakoulunkatu 3, 33720 Tampere, Finland*
[2]*School of Electrical and Information Engineering, University of the Witwatersrand, Johannesburg, 1 Jan Smuts Laan, 2001 Braamfontein, South Africa*
[3]*School of Pharmacy, PromisLab, University of Eastern Finland, Yliopistonranta 8, 70210 Kuopio, Finland*
[4]*Faculty of Information Science and Technology, Hokkaido University, Kita 14 Jo, Nishi 9 Chome, Kita-ku, Sapporo, Hokkaido 060-0814, Japan*

*E-mail: craig.carlson@tuni.fi

Received November 14, 2023; revised January 15, 2024; accepted January 22, 2024; published online February 6, 2024

In prior work, rough handling of oral tablets had been observed to drastically speed up their disintegration in water. The purpose of this study was to confirm or refute that the formation of internal microscopic fractures during rough handling is the underlying mechanism. Impacted and control tablets were subjected to micro-computed tomography and to brightness-mode ultrasound. The former revealed fracturing with a maximum crack width of 14 μm. The latter revealed strong acoustic response from the internal structure of the impacted tablets. These results confirm the hypothesis. Disintegration speed is used as a quality control mechanism after tablet manufacturing and transportation.

Oral pharmaceutical tablets comprise compressed powders.[1)] After the pois compaction process,[2)] the presence of microscopic gas pockets has been observed inside tablets[3)] that are released during disintegration in water.[4)] The pulsation behaviour of tablet gas micropockets in an ultrasound field has been associated with rapid ultrasound-assisted tablet disintegration.[5,6)] Disintegration time has been of interest for quality checks during the manufacturing process.[7)] The acoustic amplitudes during tablet monitoring must be less than the inertial cavitation threshold,[8–12)] to prevent the formation of free radicals[13)] and the deposition of heat.[14,15)]

In a prior study, it was reported that tablet disintegration is accelerated after rough handling of tablets.[16)] In this study, we investigated if rough handling visibly alters the internal structure of the tablets. Microtomography is a common methodology to study internal structures of materials.[17–20)]

Throughout this study, microcrystalline cellulose was used, as this is a commonly used tablet matrix material.[21)]

Avicel PH102 microcrystalline cellulose powder (Agro Ireland Limited, Cork, Ireland) underwent controlled compaction as previously described.[16)] The resulting tablets each had a mass of 0.4 g, a diameter of 10 mm, and a height of 4.4 mm. Rough handling was ensured by using a *tool of hard knocks*, subjecting seventy tablets to a nut drop in a controlled procedure.[16)] Nut drops were recorded with a FASTCAM MC1 high-speed camera (Photron (Europe) Limited, West Wycombe, Bucks, United Kingdom) with an 8–50 mm zoom lens (Waveshare Electronics, Shenzhen, China). A typical example of a nut drop is shown in Fig. 1.

A representative tablet that had been subjected to impact and a control tablet were prepared for micro-computed tomography, by fixating them in a customised scaffold of acrylonitrile butadiene styrene cuboids. The scaffold was positioned in the centre of a rotating plate inside a MICROXCT-400 device (Carl Zeiss AG, Oberkochen, Germany). The tomographic imaging procedure was similar to those previously described.[22,23)]

The X-ray source was operating at a power of 10 W and at a peak voltage of 60 kV. An exposure time of 1 s was set per image, whilst a detection scintillator with a 4× objective was being used. A total number of 1601 projections were acquired, evenly distributed over 360°. The resulting voxel size corresponded to $2.8 \times 2.8 \times 2.8$ μm^3. Three-dimensional images were reconstructed from the raw data by making use of XMRe-constructor 8.1.6599 software (Zeiss). These images were converted to Tag Image File Format for further processing and measurement with ImageJ 1.53t (National Institutes of Health, Bethesda, MD, USA) software.

A number of ten impacted tablets and ten control tablets were subjected to brightness-mode ultrasonography by operating a similar setup as used in prior experiments.[6,16)] An HFL38x 13–6-MHz linear probe of a SonoSite® M-Turbo® sonography device (FUJIFILM SonoSite, Inc., Bothell, WA, USA) was clamped vertically such that its face directed towards a 1-SHP coin reflector that had been fixed on the bottom of a 1220 Arctic box container (Plast 1 A/S, Hørsholm, Denmark) of $115 \times 115 \times 55$ mm^3 outer dimensions.

The vertical distance between the probe face and the reflector was 14 mm. Before each experiment, the container was filled with degassed purified water whose temperature was measured to be 18 °C. During sonication, a tablet was manually placed on top of the reflector. Sonication in two-dimensional musculoskeletal pulsed brightness mode with an estimated machine-indicated mechanical index of 0.8 and a machine-indicated thermal index of 0.1 continued for 60 s. During this time, no temperature change was measured in situ. The mechanical index and thermal index are machine-indicated values that may not be related to the in-situ indices in our 250 ml volume. They have been stated for repeatability purposes. The broadband acoustic pulse was measured to have a peak-negative pressure amplitude of 3 MPa. The machine-indicated mechanical indices were confirmed by measurements in free-field conditions. Adding reflective surfaces was not observed to change the amplitudes of the short individual pulses measured.

Each experiment generated an output of 450 brightness-mode frames. These frames were processed using MATLAB® (The MathWorks, Inc., Natick, MA, USA). Our prior work showed an average swelling rate of 0.23 ± 0.04 mm s^{-1} for impacted and a swelling rate of 0.18 ± 0.01 mm s^{-1} for control tablets.[16)] In the present study we concentrated on scattering data from within the tablets under sonication.

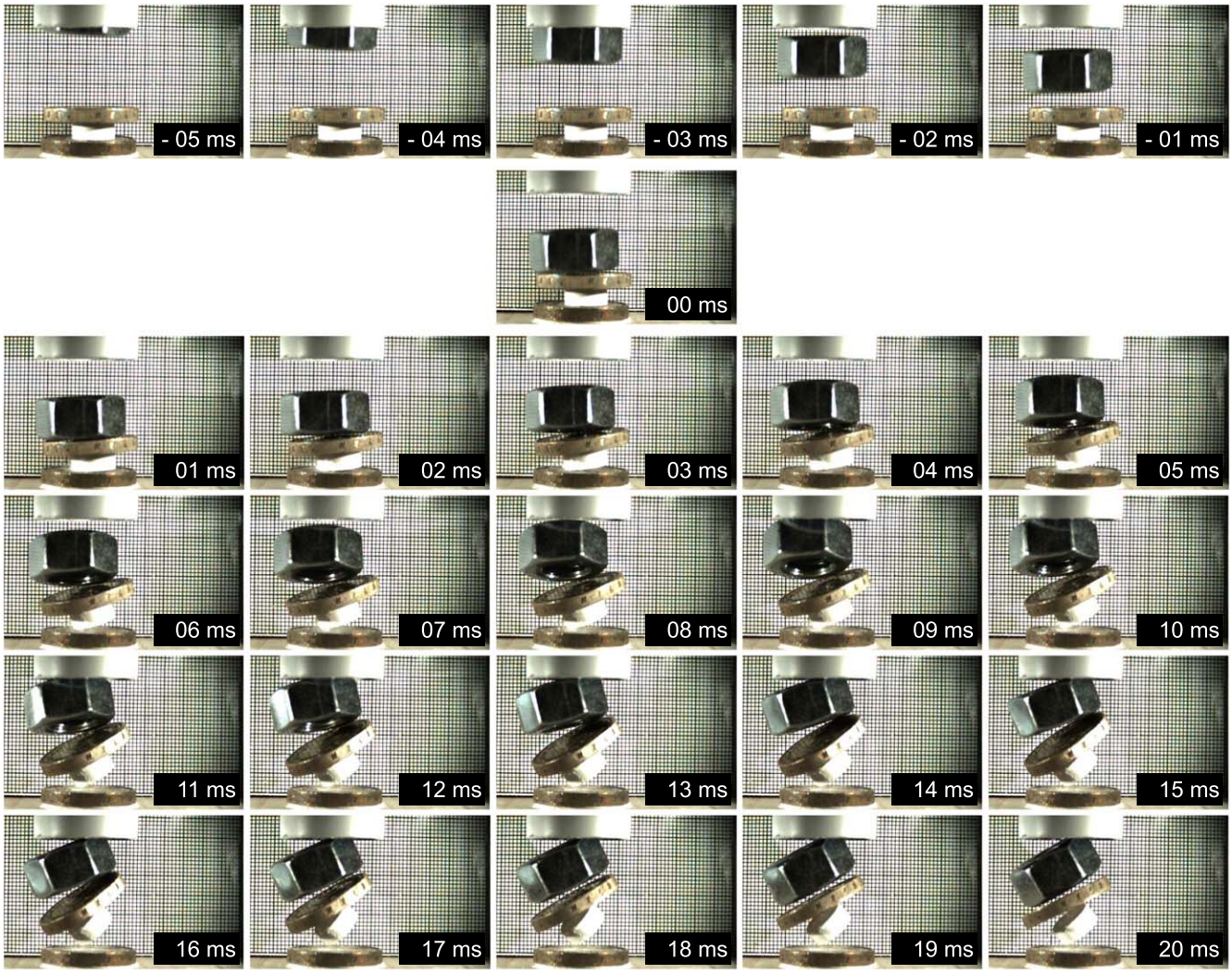

Fig. 1. High-speed video of the impact of a nut, dropped from 82 cm height, on a tablet sandwiched between two 1-SHP coins. The line density of the mesh corresponds to 1 mm^{-1}. Timestamps have been added to the lower right corners.

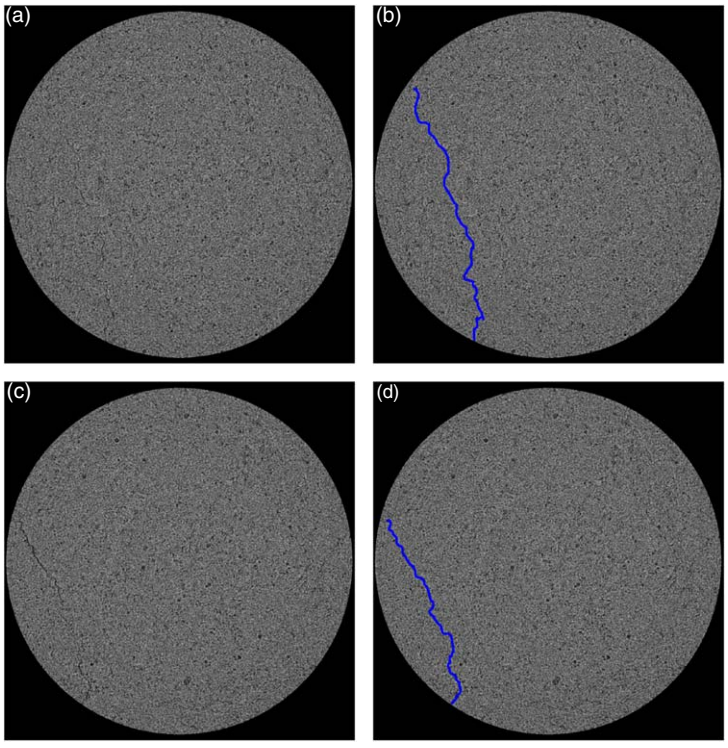

Fig. 2. Micro-computed tomography images of two x–y cross-sections of an impacted tablet at heights of $z = 1.3$ mm (a), and $z = 1.8$ mm (c). The fractures visible in the original frames (a), (c) have been highlighted in blue (b), (d).

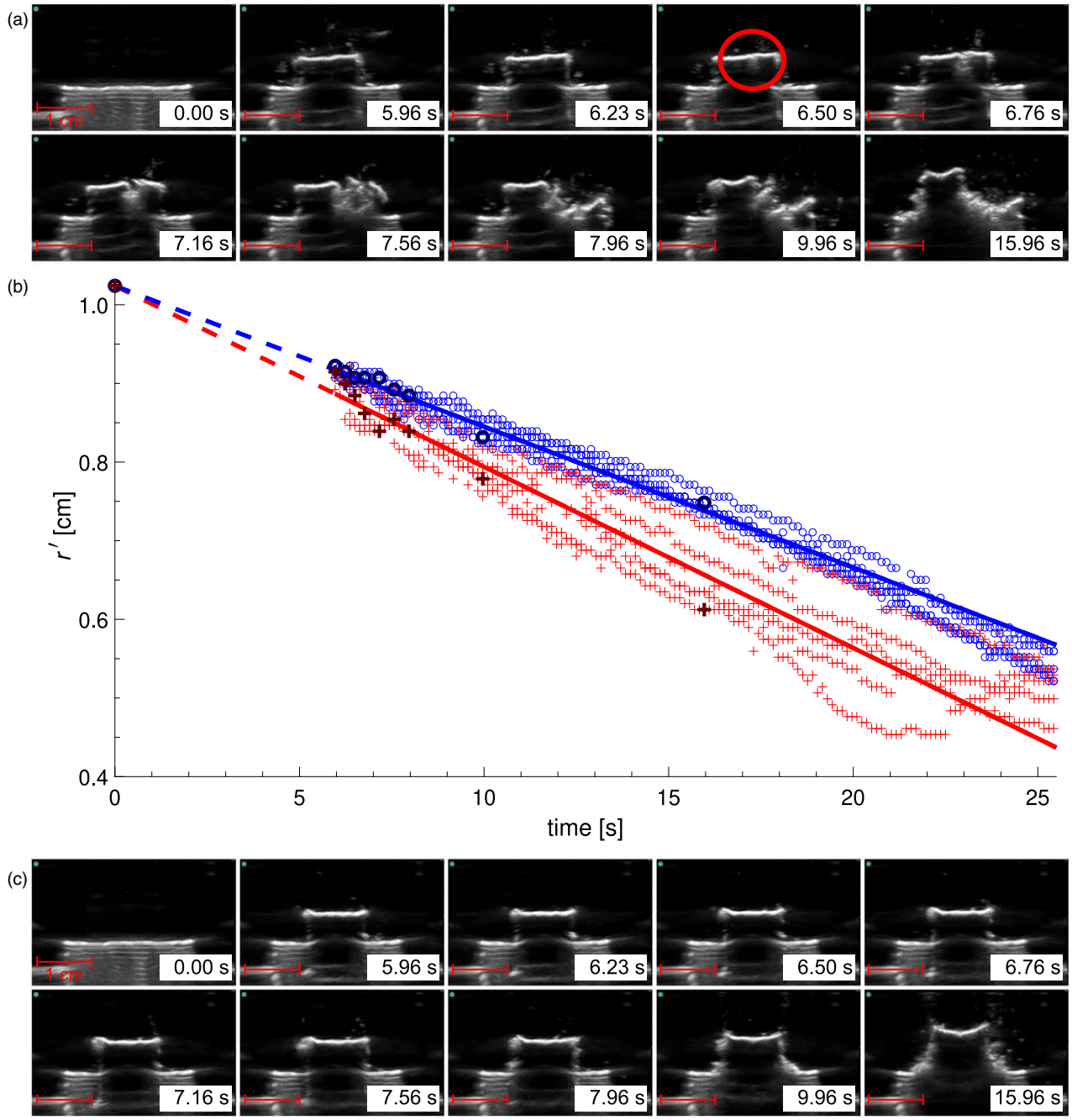

Fig. 3. Brightness-mode imaging sequences of an impacted (a) and a control (c) tablet positioned on a 1-SHP coin reflector during swelling and disintegration. The distances r' perceived between transducer and tablet were measured from these frames and superimposed on the dataset presented in our prior study (b), [16] where impacted and control tablets are indicated by + and ○, respectively. The linear swelling rate was 0.23 ± 0.04 mm s^{-1} for impacted tablets (—), and 0.18 ± 0.01 mm s^{-1} for control tablets (—). The centre of the red circle indicates a strong acoustic response within the impacted tablet. Timestamps relative to the graph time axis have been added to the lower right corners. 1 cm scale bars have been added to the lower left corners.

Figure 2 shows two representative tomographic slices of an impacted tablet. It should be noted that the cross-sections do not cover the whole tablet but only a limited region. Thin but visible fractures can be observed to run within the tablet. The maximum width of a crack was measured to be 14 μm. In the control slices, such fractures were not visible. The fractures observed had highly irregular shapes. Therefore, measuring the crack volume of tablet fractures and the associated linear acoustic resonance frequency may prove to be challenging.

Figure 3 shows a representative brightness-mode ultrasonic imaging sequence of an impacted tablet and a control tablet positioned on a 1-SHP coin reflector during swelling and disintegration. The perceived distance measured from the frames has been superimposed on the dataset presented in our prior study.[16] The internal structure shows a strong acoustic response of the impacted tablet compared to the control. Its disintegration was observed to commence from the location of strongest acoustic response. We interpret this internal region of strongest acoustic response

to coincide with the region of internal fracturing from the impact the tablet had been subjected to. It should be noted that ultrasound has been used in this study to speed up tablet disintegration and the measurements thereof. It has not been intended to represent actual in vivo situations.

As for the mechanism behind the accelerated disintegration of fractured tablets, there is room for speculation. A straightforward explanation is that the fracture connects microscopic air pockets, speeding up the water absorption of the tablet after initial water ingress. The influence of electromagnetic fields on the hydrophobicity of the compacted power has not been taken into account.

In conclusion, micro-computed tomography and brightness-mode ultrasound revealed microscopic fractures inside impacted tablets. Additionally, brightness-mode ultrasound images revealed a strong acoustic response from the internal structure of the impacted tablets. These results confirm the hypothesis that the formation of internal microscopic fractures during rough handling is the underlying reason for their accelerated disintegration in water. Disintegration time is used as a quality control test after tablet manufacturing and transportation.

Acknowledgments This work was supported by JSPS KAKENHI, Grant Nos. JP17H00864 and JP20H04542, by the National Research Foundation of South Africa, Grant No. 127102, by the Academy of Finland, Grant No. 340026, and by the Deutsche Forschungsgemeinschaft (DFG) Emmy-Noether Programme, Grant No. 38355133.

ORCID iDs Craig S. Carlson https://orcid.org/0000-0003-1059-1601 Michiel Postema https://orcid.org/0000-0001-5887-1739 Nicole Anderton https://orcid.org/0000-0001-7114-2231 Markus Hannula https://orcid.org/0000-0002-4485-8004 Joona Sorjonen https://orcid.org/0009-0006-6448-1159 Nobuki Kudo https://orcid.org/0000-0003-3463-3714 Jari Hyttinen https://orcid.org/0000-0003-1850-3055 Jarkko Ketolainen https://orcid.org/0000-0002-7636-0737

1) J. T. T. Leskinen, S.-P. Simonaho, M. Hakulinen, and J. Ketolainen, Int. J. Pharm. **442**, 27 (2013).
2) M. Sim, M. Kim, K. Ha, and J. Kim, Jpn. J. Appl. Phys. **58**, SGGB02 (2019).
3) C. S. Carlson, M. Hannula, and M. Postema, Curr. Dir. Biomed. Eng. **8**, 41 (2022).
4) N. Anderton et al., Curr. Dir. Biomed. Eng. **9**, 25 (2023).
5) Y. Zhou, N. Gu, and F. Yang, Int. J. Pharm. **586**, 119615 (2020).
6) C. S. Carlson, N. Anderton, A. Pohl, A. J. Smith, N. Kudo, and M. Postema, Jpn. J. Appl. Phys. **61**, SG1030 (2022).
7) D. Markl and J. A. Zeitler, Pharm. Res. **34**, 890 (2017).
8) T. Uchida, H. Sato, S. Takeuchi, and T. Kikuchi, Jpn. J. Appl. Phys. **49**, 07HE03 (2010).
9) T. Uchida, S. Takeuchi, and T. Kikuchi, Jpn. J. Appl. Phys. **50**, 07HE01 (2011).
10) R. Takagi, S. Yoshizawa, and S. Umemura, Jpn. J. Appl. Phys. **50**, 07HF14 (2011).
11) G. Kang, J. S. Huh, and M. J. Choi, Jpn. J. Appl. Phys. **56**, 07JC08 (2017).
12) T. Uchida, Jpn. J. Appl. Phys. **60**, SDDD04 (2021).
13) T. Aikawa and N. Kudo, Jpn. J. Appl. Phys. **60**, SDDD13 (2021).
14) T. Moriyama, S. Yoshizawa, and S. Umemura, Jpn. J. Appl. Phys. **51**, 07GF27 (2012).
15) N. Obara, S. Umemura, and S. Yoshizawa, Jpn. J. Appl. Phys. **60**, SDDE04 (2021).
16) C. S. Carlson et al., Proc. 44th UltraSonic Electronics Symp. 2023, p. 2P2–4.
17) K. Mizuno, K. Yamashita, Y. Nagatani, and M. Matsukawa, Jpn. J. Appl. Phys. **50**, 07HF19 (2011).
18) S. Koike et al., Jpn. J. Appl. Phys. **52**, 096602 (2013).
19) L. N. Q. Huy, C.-Y. Lin, and C.-C. A. Chen, Jpn. J. Appl. Phys. **61**, 071005 (2022).
20) L. N. Q. Huy and L. N. Q. Hoa, Jpn. J. Appl. Phys. **62**, 056502 (2023).
21) G. Thoorens, F. Krier, N. Leclercq, B. Carlin, and B. Evrard, Int. J. Pharm. **473**, 64 (2014).
22) J. Virta et al., Sci. Rep. **10**, 13164 (2020).
23) E. Nurkkala, M. Hannula, C. S. Carlson, A. Hopia, J. Hyttinen, and M. Postema, Curr. Dir. Biomed. Eng. **9**, 5 (2023).